Matematisk-fysiske Meddelelser
udgivet af
Det Kongelige Danske Videnskabernes Selskab
Bind **33,** nr. 8

Mat. Fys. Medd. Dan. Vid. Selsk. **33,** no. 8 (1962)

# RANGES OF RECOIL IONS FROM $\alpha$-REACTIONS

BY

LISE BRYDE, N. O. LASSEN AND N. O. ROY POULSEN

København 1962
i kommission hos Ejnar Munksgaard

# CONTENTS



## Synopsis


The recoil $Ga^{66}$ ions, produced in $(\alpha, n)$ reactions when a thin copper layer is bombarded by $\alpha$-particles from the cyclotron, are stopped in a pure gas. The thermalized ions are collected by means of an electric field, and from measurements of the activity distribution on the collector electrode the range distribution is obtained. In each gas, $H_2$, $D_2$, He, $N_2$ or A, the mean range is found to be nearly proportional to the energy E in the interval $0.6\ \text{MeV} < E < 1.2\ \text{MeV}$, in agreement with a theoretical formula given by Lindhard and Scharff. In this energy interval both electronic and nuclear stopping are of importance.

The reliability of the method is discussed. The shape of the range distribution in $H_2$ is compared with the calculated shape to be expected as a result of neutron emission from the compound nuclei, and from the half widths in various gases estimates of the straggling are obtained.

In a special experiment the range of $Ga^{66}$ ions in copper is estimated. In other measurements the ranges of potassium ions in argon and $F^{18}$ ions in nitrogen are obtained by the collector method. Gallium and potassium ions are found to be positive when thermalized, whereas $F^{18}$ in nitrogen are found to be predominantly negative.



Printed in Denmark
Bianco Lunos Bogtrykkeri A-S

## 1. Introduction

The total charge $z^*$ of a heavy ion moving through matter is determined by a balance between electron capture and loss processes[1,2]. A convenient, though not accurate, rule of thumb is the Bohr formula

$$z^* = z^{\frac{1}{3}} \cdot \frac{v}{v_0}, \tag{1}$$

where $z$ is the nuclear charge, $v$ the velocity of the ion, and $v_0 = 2.2 \times 10^8$ cm/sec is the orbital velocity of the hydrogen electron. For fast ions like fission fragments the mean charge is high at the beginning of the path, but low at the end. Accordingly, the energy loss caused by electronic encounters decreases along the range, and near the end it becomes smaller than the loss caused by nuclear collisions, which increases towards the end. The total charge depends on the stopping substance[3]. The variation of the charge with velocity and stopping substance makes range calculations rather difficult, and experimental data on range energy relations for heavy ions will always be of great value. This may be especially true for particles with an initial velocity $\sim v_0$, for which electronic and nuclear stopping may be of the same order of magnitude.

When a heavy particle is moving either through hydrogen or through deuterium, the average total charge corresponding to a given velocity must be expected to be the same in both gases and, consequently, the electronic stopping is the same[4]. The nuclear stopping, however, is smaller in $D_2$ than in $H_2$. Therefore the range of fission fragments is longer in $D_2$ than in $H_2$[5]. Since the difference stems from the part of the path where $v \lesssim v_0$, the relative difference should be greater for particles with an initial velocity of the order of $v_0$. Such particles may be obtained by bombarding medium heavy elements like copper with $\alpha$-particles of 20 MeV, which is the energy of our cyclotron beam. If a thin copper foil is used as a target, the compound nucleus, produced when a copper nucleus is hit, will be expelled from the foil and move in the forward direction with the center of mass velocity. It was anticipated that the study of the range of such recoil par-

ticles in different gases might yield valuable information regarding the relative importance of the nuclear and electronic stopping.

Experiments of that kind were earlier made by HARVEY, DONOVAN, MORTON, and VALYOCSIK[6]. These authors measured ranges in various gases of recoil ions from the reaction $Ra^{226}$ $(\alpha, 4n)$ $Th^{226}$, using 40 MeV $\alpha$-particles. They found a slightly smaller range in $D_2$ than in $H_2$; this is opposite to the case of fission fragments, but the recoil Th-ions have velocities much smaller than $v_0$, and such low velocity particles may be assumed to behave in a different way[2, 8].

By a method very similar to that of HARVEY et al. we measured ranges in $H_2$, $D_2$, He, $N_2$, and A of $Ga^{66}$ ions from the reaction

$$^{63}_{29}\mathrm{Cu} + {}^{4}_{2}\mathrm{He} \rightarrow {}^{67}_{31}\mathrm{Ga}^{*} \rightarrow {}^{66}_{31}\mathrm{Ga} + {}^{1}_{0}n, \qquad (2)$$

using $\alpha$-particles of 10, 13, and 19.6 MeV, corresponding to average ion energies of 0.61, 0.79, and 1.19 MeV, respectively, or average ion velocities of 1.32, 1.50, and $1.84 \times 10^8$ cm/sec, respectively. Also, ranges of potassium ions in argon and $F^{18}$ ions in nitrogen were measured. By another method the range of $Ga^{66}$ ions in copper was estimated.

In the next section, the experimental arrangement will be described, and in section 3 the reliability of the method is discussed. In section 4, the results of the $Ga^{66}$ measurements in gases are given and discussed, section 5 deals with the Ga range in copper, and section 6 with the ranges of K and $F^{18}$ ions. Finally, in section 7, the widths of the Ga range distributions and the angular distribution will be discussed.

## 2. Experimental method and apparatus

Formula (1) is not valid for very small velocities, and the charge is not zero at the end of the path. It is well known from the standard way of producing, for instance, a ThB deposit, that recoil ions from some $\alpha$-disintegration processes are positively charged when brought to rest in a gas. The present method is based on the fact that the $Ga^{66}$ ions will also be positive when stopped, so that they can be collected on a negative electrode.

Since the $\alpha$-beam from the Copenhagen cyclotron was used for these experiments only 1–2 hours per day, the experimental apparatus had to be made in a way which would allow the beam to be used for other pur-

poses the rest of the time. The recoil chamber was made so that it could be placed inside an existing scattering chamber and easily removed again after use. Apart from the fact that this arrangement was decisive for some of the dimensions, the special construction features implied by it are of no interest here, and Fig. 1 only shows the principal features.

The $\alpha$-beam was stopped down to a diameter of 7 mm by a lead diaphragm 10 cm from the entrance window of the chamber. The window was 10 mm in diameter; it was made of a 1.2 mg/cm$^2$ plastic foil with a thin layer of copper on the inside surface, which served as the target. The

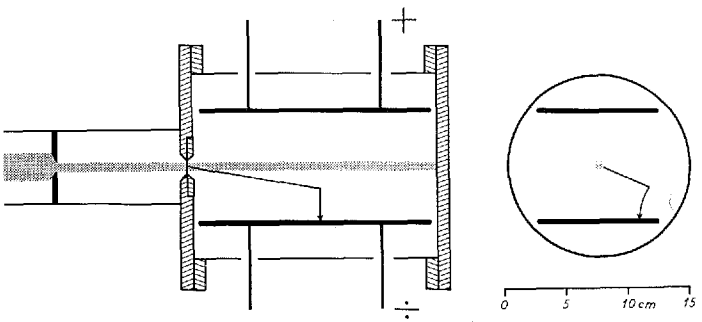


Fig. 1. Experimental apparatus.

layer, which was deposited on the plastic by evaporation in vacuo, was transparent and in some cases so thin that it was hardly conducting; the thickness was estimated from the amount of copper used and the geometry of the evaporation chamber. The uncertainty is about a factor of two. In the actual range measurements, a layer thickness of 5–10 $\mu$g/cm$^2$ was used, but occasionally a somewhat thicker layer served as the target in auxiliary experiments.

The chamber itself was a piece of a 6 inch steel tube. Inside it, there were placed two 3 mm brass plates, 10 × 19 cm$^2$, supported by Teflon insulators (not shown). One plate was held at +V volts, the other at −V volts. In some cases, the negative plate was replaced by a semicircular rod, 2 cm in diameter; the positive plate was then earthed like the rest of the chamber. V was chosen somewhat below breakdown potential, different for different gases and pressures. It ranged from 200 to 2000 volts. The ionization currents, of the order of 20–100 $\mu$A, were used by the cyclotron operator to maintain the machine at optimum conditions. The $\alpha$-current itself which was not measured, was of the order of 0.05 $\mu$A.

On the inside surfaces of the plates grooves were cut lengthwise and crosswise; they were spaced 1 cm and formed a whole quadratic coordinate net. Before each experiment the plates were covered with aluminium foils 3 mg/cm$^2$ thick; the foils were bent round and fastened on the back sides by means of adhesive tape. By cautiously sliding a stick along the grooves the coordinate lines were transferred to the foils. After each bombardment the aluminium foils were cut along the lines, and the activities of the pieces were measured.

The chamber was filled with a pure gas. Before and after the bombardment the pressure was measured on a mercury gauge. The connection to the manometer was via a stopcock and, to avoid any possible influence of mercury vapour, the stopcock was opened only a few seconds and precautions were taken to have the main gas flow always going towards the manometer. When He was used, the chamber was connected to a liquid air charcoal trap. The other gases were continuously circulated through a side tube with hot calcium. This is a well working, standard procedure for the purification of A. For $H_2$, $D_2$, and $N_2$ special precautions had to be taken. When using these gases the temperature of the calcium was kept below a certain value (not known on an absolute scale), and before the actual experiments the calcium was saturated with the gas at the proper pressure and the temperature to be used. Separate purifiers were used for each gas.

The radioactivity of the aluminium pieces were measured by a 1 1/2 × 1 1/2 inch NaJ crystal. Each little piece of aluminium could be put in its own small specimen tube and pressed down against the flat bottom by a weight. During the counting the specimen tube was kept in a standard position right on top of the crystal by means of a holder. Small corrections had to be applied because the bottoms of the various specimen tubes were slightly different; corrections for decay were also applied. Often several aluminium pieces, for instance the 10 pieces from a whole row, were put in the same specimen tube. To speed up the counting four counter sets were used, each consisting of the crystal, the photomultiplier, the amplifier, and a single channel analyzer.

Reaction (2) was chosen, among other reasons, because $Ga^{66}$ is a convenient nuclide, its half-life being 9$^h$, which leaves plenty of time for counting; its $\gamma$-spectrum contains rather strong high energy lines, and by simply using a bias of 1.7 MeV one can avoid counting almost any other possible activity. $Na^{24}$ might be produced by high energy neutrons in the aluminium, but it was not found in significant amounts.

The other activities ($K^{42}$, $K^{43}$, and $F^{18}$) were measured with a properly chosen single-channel window, selecting a suitable $\gamma$-line. For the adjustment standard sources of $Co^{60}$ (1.17 and 1.33 MeV), $Cs^{137}$ (0.66 MeV), and $Na^{22}$ (0.51 MeV) were used.

## 3. Discussion of the method

One might consider the following questions:

1. Will the $Ga^{66}$ ions remain positive when stopped down to thermal velocities? Or will some be positive, some negative, and some neutral? Or will a particular ion have a fluctuating charge? It is clear that the collection along the electric field lines can only be good when the ions, after being thermalized, remain positive (or negative). If the ions are sometimes neutral, they will diffuse around, and the distribution will be smeared out.
2. If the ions are positive, will there still be some diffusion?
3. If the collection works well, what is the influence of the inhomogeneity of the field?
4. Will the ions, when collected on the aluminum foil, stick to the spot, or is it possible that they may again be liberated as neutral atoms?

The $\alpha$-particles produce of the order of $10^{15}$ ion pairs per sec. If the electrons attach themselves to some impurity molecules to form negative molecular ions, some risk exists that they may collide with $Ga^{66}$ ions and neutralize them. One reason for using very pure gases is to avoid attachment and to secure a fast removal of the negative ions. Other reasons are that, in pure gases, it is reasonable to expect[7] that clustering does not occur, that charge exchange reactions between thermal $Ga^{66}$ ions and molecules can be neglected, and that the positive ion collection time is only a fraction of a milli-second, so that diffusion will be completely unimportant. Furthermore, an important reason is that possibly the fast $Ga^{66}$ ions may have a mean charge and a mean range depending somewhat on even rather small impurity admixtures.

It was found that more than 90 per cent of the $Ga^{66}$ activity was collected on the negative plate when the voltage was sufficiently high. Less than 5 per cent was found on the positive plate and less than 5 per cent on the walls of the chamber. As shown in Figs. 2 and 3, the activity on the negative plate was distributed in a rather broad peak, but this was to be expected, because the neutrons emitted from the compound $Ga^{67}$ nuclei

will give the $Ga^{66}$ nuclei recoil momenta varying in direction and magnitude. In fact, calculations which will be more closely discussed below, indicate that the width caused by neutron recoil is comparable to the experimental width found in the light gases. Experience thus seems to show that the method works for $Ga^{66}$.

In Fig. 2 are plotted the $Ga^{66}$ activities of the aluminium pieces against

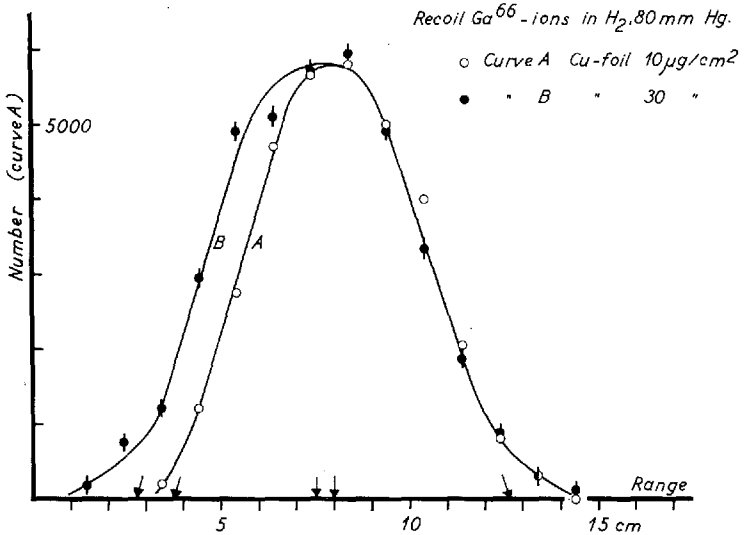


Fig. 2. Distribution of $Ga^{66}$ activity along the negative collector plate for two thicknesses of the Cu layer and with the chamber filled with $H_2$ to a pressure of 80 mm Hg (23° C).

their positions along the collector plate. The ten pieces from each row are added. The abscissae are the distance from the window as measured in the beam direction. Since some particles diverge they will actually have travelled longer. The mean value as determined from the curve therefore is the mean of the projection of the ranges, and not the mean of the ranges themselves. The difference will be only a few per cent and can be neglected (cf. section 7). It may be emphasized that we are here talking about a purely geometrical effect, neglecting the influence of scattering in the gas. The latter phenomenon implies that the total path length, especially in the heavier gases, will be longer than the range, and this difference may be of much larger magnitude.

Fig. 2 gives further evidence for the reliability of the method. It should be

expected that curve B obtained with the thicker target would follow the thin target curve A on the right side, because the thick target may be considered to be made up of a stack of thin targets, but, on the left side, B would be displaced against smaller range values, in qualitative agreement with the figure. Since the mean range in copper is about 270 $\mu g/cm^2$ (see section 5), the displacement should be about $\frac{30-10}{270} \times 8 \sim 0.6$ cm, 8 being

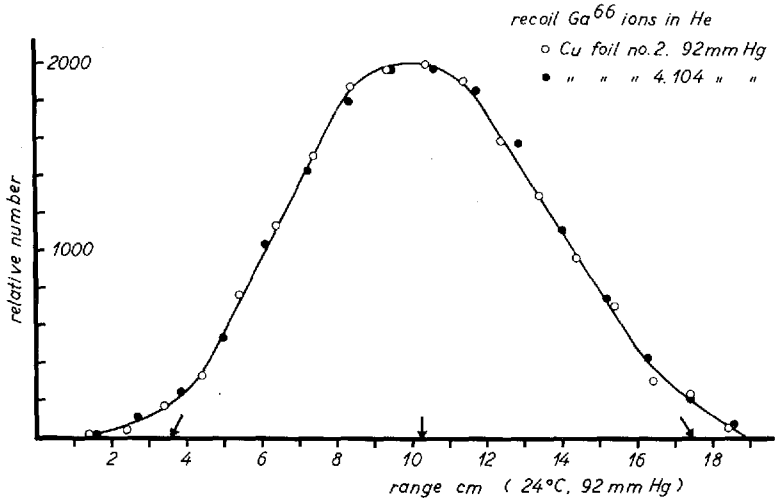


Fig. 3. Distribution of $Ga^{66}$ activity along the negative collector plate when using a thin Cu layer (5–10 $\mu g/cm^2$) and He as stopping gas.

the mean range as obtained from curve A. The displacement is slightly larger, $\sim 1$ cm, but since neither the thickness nor the range in copper is accurately known, the quantitative agreement is not too bad. It is also inferred that, when a target thickness not exceeding 10 $\mu g/cm^2$ is used, the target contributes only little to the width of the distribution.

Fig. 3 shows the result of two measurements in He. Two different copper layers of about equal thickness ($\sim 10$ $\mu g/cm^2$) and two He-pressures were used. Within a few millimeters the two sets of points show the same distribution. Here it might have been more convincing if the difference between the two pressures had been greater. However, in each experiment the pressure was purposely chosen in such a way that the peak fell not too far from the middle of the chamber where the electric field has no component in the

$\alpha$-beam direction. Towards the end of the plates the field inhomogeneity will distort the results, and the lower parts of the curves — in Fig. 3 to the left of $\sim 4$ cm and to the right of $\sim 16$ cm — do not reflect accurately the actual range distributions.

The distribution curves were the same whether obtained with the collector plate or with the semi-circular rod. All evidence thus indicates that the longitudinal distributions may be regarded with some confidence.

On the contrary, lateral distributions measured by means of the activity on the plate are of no value. Even though the positive ions are rather quickly removed, the large number of them will create a space charge which will distort the electric field in a way as sketched in Fig. 4a. In Fig. 4b the black points and the full drawn curve show the activity of the 10 aluminium pieces in the row corresponding to the mean range. The appearance of the curve may be understood by help of Fig. 4 a. One consequence of the field distortion is the large broadening of the curve, demonstrated by comparison with the dotted curve and the white points which were obtained in the following way: 20 mm behind the window a circular lead disk, 10 mm in diameter, was placed; it stopped the beam as well as the recoil ions moving nearly forward. The dotted curve gives the activity distribution along the same row of aluminium pieces as before, but now there is no positive space charge. For the latter curve the central dip is due to the missing recoil ions in the forward directions, and the shape of the curve agrees with rough calculations. For the former curve the central dip is, at least mainly, a consequence of the field distortion.

The field distortion by space charge will have no influence on the longitudinal distribution. However, in order to measure the latter correctly, some knowledge of the lateral spread is necessary, because it has to be avoided that the recoil ions strike the plates before being thermalized in the gas. The dotted curve in Fig. 4b gives some information on the lateral spread and indicates the fulfilment of this requirement. Further indication was obtained in experiments where the plates were removed and the end flange of the chamber was covered with two aluminium foils. During bombardment the chamber was evacuated. Afterwards the foils were cut into circular rings by means of especially prepared punches, and the activities of the rings were measured. Fig. 5 shows the $Ga^{66}$ activity on the catcher foil. The underlying foil was inactive (only $\gamma$-energies $> 1.7$ MeV were measured) with the exception of the innermost circle which was hit by the $\alpha$-beam. For this circle the two foils were about equally active, but since it may not be justified

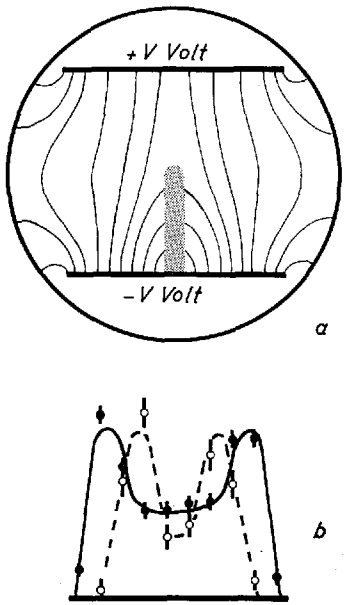


Fig. 4. a) Distortion of the electric field due to positive space charge (shaded area in the figure). Cross section perpendicular to the beam direction. Qualitative sketch. – b) Distribution of $Ga^{66}$ activity across the negative plate. Full drawn curve under normal conditions, dotted curve when the beam and the recoil ions at small angles are stopped.

to use the difference between the activities of the two circles as a measure of the $Ga^{66}$ nuclei from the copper layer*, the latter could not be determined for the innermost circle.

In Fig. 5 curve b gives a reasonably good fit to the experimental points. The integral curve e shows the percentage of the total number of particles within a cone of half angle $\theta$ equal to the abscissa. It may be seen that 85% of the recoils emerge from the target foil with $\theta < 12°$, and if the angular distribution were not changed by the stopping gas the full length of the chamber could be used without fear of distortion due to particles being lost by striking the plates. In all actual range measurements only the tail of the distribution curves were allowed to exceed a distance of some 13—14 cm from the foil. In argon, where the scattering is largest, the mean range was kept below 9 cm, and it is believed that a negligibly small amount of recoils was lost.

* Some of the active nuclei produced in the first foil will be thrown into the next foil, which, in the absence of $Ga^{66}$ from the copper target, would have the higher activity.

Attempts were made to measure the angular distribution with gas in the chamber. An aluminium covered plate was placed perpendicular to the beam at a distance from the target foil corresponding to the mean range, and again the activity of 6 mm wide rings was measured. Curves obtained with and without $H_2$ were almost identical and in fairly good agreement with the distribution to be expected according to Fig. 5. In A the distribu-

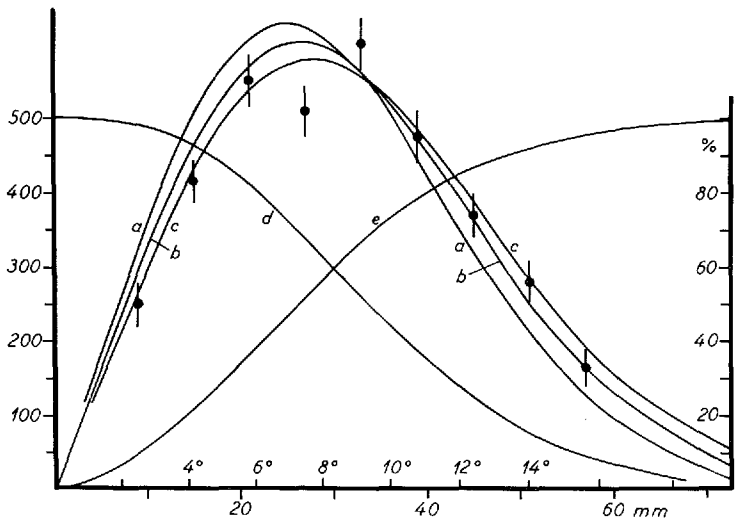


Fig. 5. Radial distribution of $Ga^{66}$ activity on the end flange of the evacuated recoil chamber. The $Ga^{66}$ was produced by bombarding Cu with 19.6 MeV $\alpha$-particles. The abscissa is the radial distance from center. A scale showing the projection angle $\theta$ of the ions is also given. The points show the activity in relative units on circular rings, each 6 mm wide. a, b, and c, are calculated curves to be discussed in section 7, p. 26. They show the $I(\theta)\,d\theta$ distribution. Corresponding to b, curve $d$ shows the $I(\theta)\,d\omega$ distribution, and curve $e$ the integral $\int_0^\theta I(\theta)\,d\theta$.

tion was much broader; the measurements were not completely reproducible, perhaps because, since the actual collector plates were removed, no sufficiently good electric field was applied, and hence some $Ga^{66}$ atoms stopped in the gas may have reached the end plate by diffusion. However, the measurements showed that less than 4% of the activity on the catcher foil was found at radii larger than 45 mm.

Before leaving the discussion of the method of collecting the recoil ions it may be mentioned that reproducible results were obtained only when the aluminium foils were handled with utmost care. By experiment it was found that 40—80% of the activity could be removed from the foil 1) by dipping

it in water or ethyl alcohol, 2) by rubbing it with a wet cloth or 3) by pressing a thumb against it. 20—40% was removed 1) by rubbing lightly with a clean, dry cotton wool cloth or 2) by touching gently with a clean, dry finger. Here is another reason for using a pure and dry gas. There may also be some reason for using as collector foil the aluminium which is chemically related to gallium.

## 4. Range of $Ga^{66}$ ions in gases

Longitudinal distributions of $Ga^{66}$ activity obtained in $H_2$, $D_2$, He, and A are shown in Fig. 6.

The difference in ranges in $H_2$ and $D_2$ demonstrates at once the importance of nuclear stopping, as discussed in the introduction. It also tells something about the electronic stopping.

For the velocity loss per cm due to nuclear encounters Bohr has given the formula (ref. 2, (5.1.2.))

$$-\frac{dv}{dx} = 2\pi N \frac{z_1^2 z_2^2 e^4}{m_1 m_2 v^3} L_v \tag{3}$$

with

$$L_v = \log\left\{ z_1 z_2 \sqrt{z_1^{2/3} + z_2^{2/3}}\, \frac{\mu (m_1 + m_2)}{m_1 + m_2} \cdot \left(\frac{v_0}{v}\right)^2 \right\}^{-\frac{1}{2}},$$

where N is the number of atoms per $cm^3$, $m_1$ and $z_1$ are the mass and nuclear charge numbers of the ion, $m_2$ and $z_2$ the corresponding values for the stopping substance, $v$ is the ion velocity, and $\mu$ and $e$ are the mass and charge of the electron. In a way described earlier (ref. 4, p. 31) the range energy relations in $H_2$ and $D_2$ may be calculated, assuming no electronic stopping. For $Ga^{66}$ ions of velocity $1.84 \times 10^8$ cm/sec the range in $D_2$ would be 1.38 times the range in $H_2$. The experimental ratio is 1.17, thus indicating the importance of both electronic and nuclear stopping.

According to formula (3), the nuclear stopping power per cm will be about the same in $D_2$ and in He. The longer range in He shows again that the electronic stopping in $D_2$ is not negligibly small compared to the nuclear stopping. It shows furthermore that the electronic stopping is smaller in He than in $D_2$. In this connection it is interesting to remember that the total charge of fast fission fragments is smaller in He than in $H_2$ (or $D_2$)[3]. How-

ever, from the present measurements no conclusion regarding the ion charge in $D_2$ and in He can be drawn, because the range may be longer in He than in $D_2$ even if the charge values are equal. In fact, the ratio $R_{He}/R_D = 1.22$ between the ranges in He and in $D_2$ is closely the same as the ratio $\left(\frac{dE}{dx}\right)_H \Big/ \left(\frac{dE}{dx}\right)_{He} = 1.21$ between the stopping powers in $H_2$ and in He for

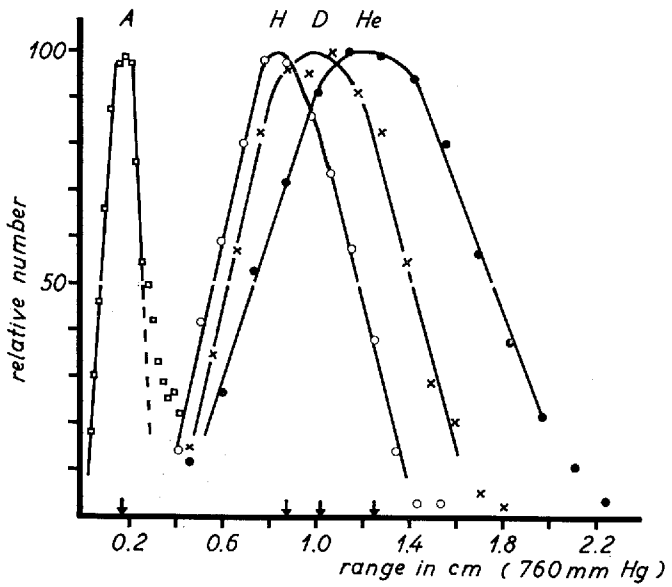


Fig. 6. Range distributions in $H_2$, $D_2$, He, and A of $Ga^{66}$ ions produced by bombarding Cu with 19.6 MeV $\alpha$-particles. The abscissa is the range in cm at 760 mm Hg and 23° C. – In the measurements the gas pressure was 71, 79, 104, and 17.3 mm Hg of $H_2$, $D_2$, He, and A, respectively.

5 MeV $\alpha$-particles. This agreement between the figures is accidental; actually, the ratio between the electronic stopping powers for these slow ions may be expected to be higher than 1.2, but the ratio between the nuclear stopping powers in He and $D_2$ is about 1, and the range ratio depends on both.

For the heavier gases nitrogen and argon the experiments give $R_N/R_A = 1.02$, and one has for 5 MeV $\alpha$-particles $\left(\frac{dE}{dx}\right)_A \Big/ \left(\frac{dE}{dx}\right)_N = 0.98$. This agreement may be understood in a somewhat similar way as for $D_2$—He.

When comparing the light and heavy gases one does not find such agreement between ratios of ion ranges and $\alpha$-ranges. The experimental value for the ratio between the ranges in A and in He is $R_A/R_{He} = 0.135$,

whereas the ratio between the stopping powers for 5 MeV $\alpha$-particles is $\left(\frac{dE}{dx}\right)_{He} \Big/ \left(\frac{dE}{dx}\right)_{A} = 0.183$, and for slower particles it may even be larger.

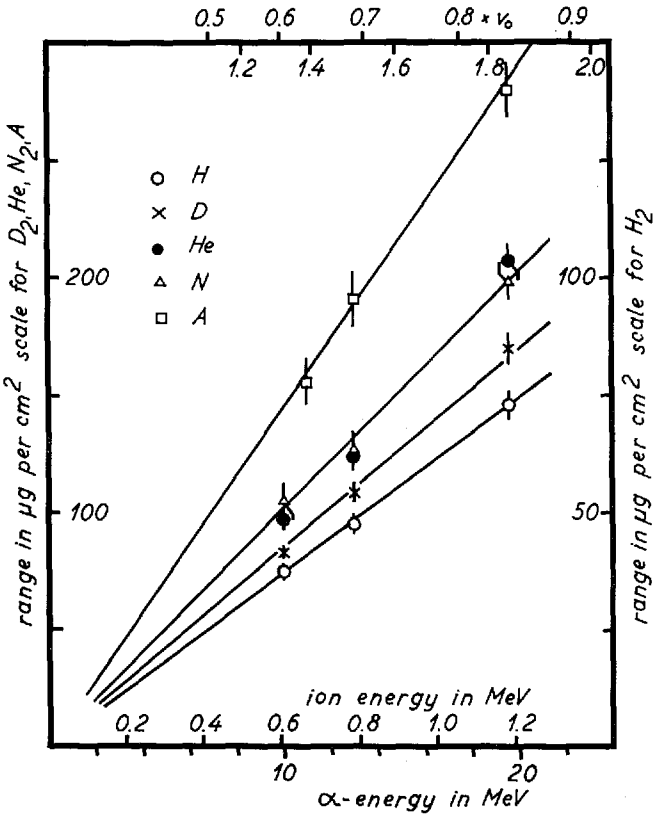


Fig. 7. Range in $\mu g/cm^2$ of $Ga^{66}$ ions in gases. Note the different ordinate scales for $H_2$ and for the other gases. The ions are produced in the reaction $Cu^{63}$ ($\alpha$, $n$) $Ga^{66}$ and the abscissa is the $\alpha$-energy. A scale showing the mean ion energy is also given. On the top of the figure scales are given for the average ion velocity in units of $10^8$ cm/sec and in units of $v_0$, the orbital velocity of the hydrogen electron.
The curves are straight lines through origo.

This again illustrates the influence of nuclear stopping which for the Ga ions, according to formula (3), is many times larger in A than in He.

Table 1 and Fig. 7 summarize the results obtained for various $\alpha$-energies. A range correction of 2% for finite target thickness has been applied. To a rather good approximation the range in each gas is found to be proportional to the energy. The proportionality constants are given in Table 2.

TABLE 1. Range in gases of recoil $Ga^{66}$ ions, given in mm (760 mm Hg, 23°C) and in $\mu g/cm^2$.

| $\alpha$-energy<br>mean ion energy<br>mean ion velocity | 19.6 MeV<br>1.19 MeV<br>$1.84 \times 10^8$ cm/sec | | | | 13.0 MeV<br>0.79 MeV<br>$1.50 \times 10^8$ cm/sec | | | | 10.0 MeV<br>0.61 MeV<br>$1.31 \times 10^8$ cm/sec | | | |
|---|---|---|---|---|---|---|---|---|---|---|---|---|
| | mm | | | $\mu g/cm^2$ | mm | | | $\mu g/cm^2$ | mm | | | $\mu g/cm^2$ |
| | 1. | 2. | av. | | 1. | 2. | av. | | 1. | 2. | av. | |
| $H_2$ | 8.8 | 9.0 | 8.9 | 73 | 5.9 | 5.7 | 5.8 | 47.6 | 4.55 | 4.62 | 4.58 | 37.6 |
| $D_2$ | 10.3 | 10.4 | 10.4 | 170 | 6.5 | 6.7 | 6.6 | 109 | 4.95 | 5.15 | 5.05 | 83 |
| He | 12.6 | 12.5 | 12.6 | 207 | 7.3 | 7.8 | 7.5 | 124 | 5.8 | 6.0 | 5.9 | 97 |
| $N_2$ | 1.76 | 1.69 | 1.73 | 199 | 1.10 | | | 127 | 0.91 | | | 105 |
| A | 1.69 | 1.71 | 1.70 | 280 | 1.16 | | | 191 | 0.95* | | | 156* |

* $\alpha$-energy 11.0 MeV.

Proportionality means, that the total stopping power $\frac{dE}{dx}$, equal to the sum, $\left(\frac{dE}{dx}\right)_e + \left(\frac{dE}{dx}\right)_\nu$, of the electronic and nuclear stopping powers, is constant in the energy range considered. Values for $\frac{dE}{dx}$ in various gases are also given in Table 2.

If the electronic stopping is neglected one should, for velocities $v \ll v_0$ just expect proportionality between range and energy (cf. formula (5.4.2) in ref. 2), while for $v \sim v_0$ one should expect a somewhat stronger energy variation (ref. 2, formula (5.3.2)). The present experiments show that both electronic and nuclear stopping play important roles, and none of them can be neglected. Now, for increasing velocities, the nuclear stopping decreases, but the electronic stopping increases and, in fact, it so happens that these two effects balance each other in such a way that, for a considerable interval of velocities, not only for $v \ll v_0$, the range is closely proportional to the energy. This is discussed by LINDHARD and SCHARFF[8] who give the formula

$$R' = k \times E \times \frac{m_2(m_1+m_2)}{m_1} \cdot \frac{\sqrt{z_1^{2/3}+z_1^{2/3}}}{z_1 z_2}, \qquad (4)$$

where the units used for the range, the energy, and the masses are $\mu g/cm^2$, MeV, and mass units, respectively, and where theoretically $k = 600$.

It is borne out by the experiments that the formula gives a rather good approximation for Ga ions even for velocities comparable to $v_0$. Intro-

TABLE 2. $R/E$, range in $\mu g/cm^2$ divided by energy in MeV, and stopping power $\frac{dE}{dx}$ in keV per $\mu g/cm^2$ for $Ga^{66}$ ions in gases.

| | $R/E$ for $Ga^{66}$ ion energies | | | $R/E$ Weighted mean | $\frac{dE}{dx}$ |
|---|---|---|---|---|---|
| | 1.19 MeV | 0.79 MeV | 0.61 MeV | | |
| $H_2$ | 61.3 | 60.3 | 61.6 | 61.1 | 16.4 |
| $D_2$ | 143 | 138 | 136 | 139 | 7.2 |
| He | 174 | 157 | 159 | 163 | 6.1 |
| $N_2$ | 167 | 161 | 172 | 167 | 6.0 |
| A | 236 | 242 | 233* | 237 | 4.2 |

* for energy 0.67 MeV.

ducing the experimental range values into the formula we find for $k$ the values given in Table 3. It may be seen that the fit is very good for $H_2$ and for $N_2$. In $D_2$ the experimental values vary monotonically with velocity, which would indicate that the relative range difference between $H_2$ and $D_2$ decreases with decreasing velocity; however, the variations are hardly outside the experimental uncertainty. The rather large $k$-values in He show that, here, the electronic stopping plays a comparatively minor role than in the other gases. The small $k$-values in A reflect the influence of scattering in the stopping gas; actually, in (4) R′ stands for the average total path length, and the average (projected) range should be expected to be smaller than the former by a factor[8] $\frac{1}{1+\frac{1}{3}\frac{m_2}{m_1}} = 0.83$, thus leading to a $k$ value of 500, in close agreement with the experiments.

TABLE 3. Experimental value of the constant $k$ in formula (4).

| $Ga^{66}$ ion velocity in units of $10^8$ cm/sec | 1.84 | 1.50 | 1.38 | 1.31 |
|---|---|---|---|---|
| $H_2$ | 580 | 570 | | 580 |
| $D_2$ | 660 | 640 | | 620 |
| He | 750 | 680 | | 690 |
| $N_2$ | 590 | 560 | | 600 |
| A | 510 | 520 | 550 | |
| Cu | 340 | | | |

## 5. Range of $Ga^{66}$ ions in copper

A copper foil of thickness about 1.5 mg/cm$^2$ was bombarded with $\alpha$-particles. A thin gold foil, thick enough to stop the recoiling $Ga^{66}$ ions, was placed close behind it. If $t$ is the thickness of the copper foil, $a_1$ its $Ga^{66}$ activity, and $a_2$ the $Ga^{66}$ activity of the gold foil, the quantity

$$R = t\frac{a_2}{a_1 + a_2}$$

may be taken as a measure of the mean range of Ga ions in copper.

Results of such measurements are shown in Fig. 9. It may be seen that the values for R are roughly proportional to the energy, and that they are not much different from the range in argon. If the R-values are multiplied by $\left(1+\frac{1}{3}\frac{m_2}{m_1}\right)$ to give the total path lengths, the latter are found to be, within 2%, the same in A and in Cu.

In Table 3 a $k$-value is given. Assuming the range to be smaller than the path length by the factor $\frac{1}{1+\frac{1}{3}\frac{m_2}{m_1}} \sim \frac{3}{4}$, the $k$-value to be expected would be ~450. However, when $m_2$ is about as large as $m_1$ just as for copper, the scattering gives rise to a very large smearing-out effect. Furthermore, the activity ratio $\frac{a_2}{a_1+a_2}$ may depend on the collector foil, which in our case was gold, i. e. a substance with a rather high $m_2$ (back scattering).

## 6. Ranges of other recoil ions

In our measurements of the $Ga^{66}$ activity we usually counted $\gamma$-rays with energies higher than 1.55 MeV. Using argon as a stopping gas it was found, however, that the range distribution had a foot on the right side. This may be seen in Fig. 6; it has only a negligible influence on the important part of the distribution curve. It is caused by a $K^{42}$ activity, half life 12$^h$, produced in the gas by the reaction $A^{40}(\alpha, np)K^{42}$. $K^{42}$ has a rather strong $\gamma$-line at 1.51 MeV. By counting, after the actual $Ga^{66}$ measurements, $\gamma$-rays in the energy interval 1.45—1.60 MeV, it was found possible to obtain the $K^{42}$ activity distribution as well as a corrected $Ga^{66}$ distribution. From the corrected $K^{42}$ distribution the range of $K^{42}$ in A was obtained.

By the reaction $A^{40}(\alpha, p)K^{43}$ also $K^{43}$ is produced. This nuclide has a half-life of 22h; it has a strong $\gamma$-line at 0.615 MeV, which could be measured several days after bombardment.

In later measurements of the $Ga^{66}$ range in A the counting limit was raised to 1.7 MeV and thus the $Ga^{66}$ activity distribution was not disturbed

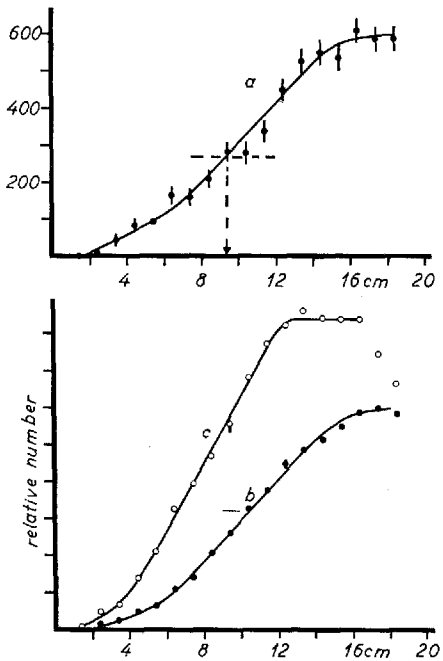


Fig. 8. Activity of $K^{42}$ (curve a) and $K^{43}$ (curves b and c) per cm of collector plate. The abscissae are the distances from the entrance window. The potassium is produced in the argon gas by $(\alpha, p)$ and $(\alpha, np)$ reactions. Curve a and b refer to the same argon pressure (17.3 mm Hg), curve c to a higher pressure (24.4 mm Hg).

by the K activity. The $K^{43}$ distribution could still be obtained as a bi-product.

Fig. 8 shows some examples of distribution curves. Since the A-target is thick, the curves are of the integral type. If the range distribution were a sharp peak, the integral curve would reach half maximum height for an abscissa equal to the (mean) range $R_m$. Assuming a Gaussian distribution with full width at half maximum height equal to $R_m$*, one finds that the ordinate for $R_m$ is not 0.5, but only 0.45 times the maximum height.

Clearly the determination of the mean range is less precise than for the

* This is a rough estimate; actually, the width may be larger (cf. section 7).

Ga ions, and the information about the width of the distribution is poor Also, the field inhomogeneity near the end of the plates may be more serious; in fact, the plateau must be reached before 15—16 cm, or the result will only be a lower limit for the mean range. For this reason the $K^{42}$ and $K^{43}$ ranges were measured in special experiments, in which no Cu-layer was

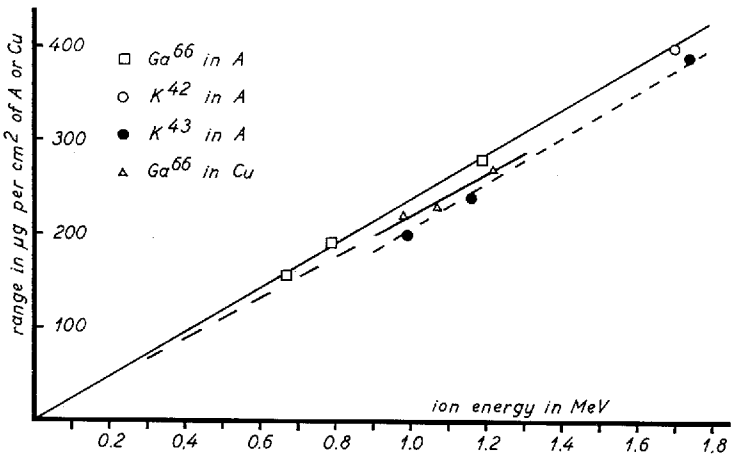


Fig. 9. Range of Ga and K-ions in A and of Ga ions in Cu.

used and the pressure was high enough to make the chamber length considerably larger than the ion range (see Fig. 8 c).

Similar experiments with no Cu-layer and with $N_2$ in the chamber yielded a value for the range of $F^{18}$ ions in $N_2$. The 511 keV line was used; the half-life of $112^m$ was observed. Some shorter living activity produced in the plastic foil was allowed to die away, and only measurements made more than 3 hours after the bombardment were used.

The K ions in A were found to go predominantly to the negative plate, the positive plate having only about 10% of the activity. Both plates gave the same distribution.

The $F^{18}$ ions in $N_2$ were found to behave in a different way, about 2/3 going to the positive plate and only 1/3 to the negative plate. The distribution on the positive plate was similar to the curve shown in Fig. 8 c. The distribution on the negative plate was probably identical, but it was measured on two other counters, and due to an accidental failure of the power supply, it was less reliable.

The different behaviour of the ions may give a hint concerning a possible

influence of the chemical nature of the ions on the ionic charge of thermal ions.

The values obtained for the ranges of K ions in A and $F^{18}$ ions in $N_2$ are summarized in Table 4. The values printed in italics were determined in particularly designed experiments and they are considered to be the most reliable.

TABLE 4. Ranges in mm (760 mm Hg, 23°C).

| $\alpha$-energy in MeV | 19.6 | | 13.0 | 11.0 |
|---|---|---|---|---|
| $K^{42}$ ions in A | 2.2 | *2.38* | 1 | |
| $K^{43}$ ions in A | 2.2 | *2.34* | 1.4 | 1.1 |
| $F^{18}$ ions in $N_2$ | | *4.09* | | |

In Table 5 the ranges in $\mu g/cm^2$ and the $k$ values to be inserted in (4) to fit the data are given. Here again $m_2 \sim m_1$, and if it were justified to use formula (4), one should expect $k \sim 450$. The small value of $k$ for $F^{18}$ ions in $N_2$ shows the non-validity of (4) for these rather fast ions ($v \sim 3.5\, v_0$). The nuclear stopping power computed from (3) would lead to a range more than 100 times larger than the experimental value, and it is thus found that for these ions the nuclear stopping is vanishingly small compared to the electronic stopping.

It may be noted that for $K^{43}$ ions the range is found to be nearly proportional to the energy, and that for equal energy the K ions and the Ga ions have about the same range (see Fig. 9). The latter is contradictory to formula (4), as is also seen from the low $k$-values. In view of the close quantitative agreement between the formula and our Ga range values in gases, it seems strange that the formula should be in error by almost a factor

TABLE 5.

| | Velocity* cm/sec × $10^8$ | Energy MeV | Range $\mu g/cm^2$ | k |
|---|---|---|---|---|
| $K^{42}$ in A | 2.79 | 1.70 | 400 | 280 |
| $K^{43}$ in A | 2.79 | 1.74 | 390 | 270 |
| $K^{43}$ in A | 2.28 | 1.16 | 240 | 250 |
| $K^{43}$ in A | 2.10 | 0.99 | 200 | 230 |
| $F^{18}$ in $N_2$ | 6.47 | 3.90 | 480 | 110 |

* Actually, the velocity of the compound nucleus which is assumed equal to the mean ion velocity.

of two for K ions which have velocities only slightly greater than the Ga ions. Neither can we imagine the experimental ranges to be so much wrong. A possible explanation for the discrepancy might be the following.

There is reason to believe that the $Ga^{66}$ ions are produced in compound nuclear reactions and that the measured mean range corresponds to an ion velocity equal to the velocity of the compound nucleus (cf. next section). We have assumed that also the $A^{40}(\alpha, p)K^{43}$ reaction takes place via a compound nucleus, but if direct interaction processes are of importance, the residual nuclei may acquire smaller mean velocities, since the protons may be emitted predominantly in the forward direction.

This explanation does not seem too plausible. We should like to point out that the cases of disagreement are those in which $m_1 \sim m_2$ (Ga ions in Cu, K ions in A).

## 7. Discussion of range distributions and angular distributions of $Ga^{66}$ ions

### Remarks on straggling and nuclear temperature

As already mentioned, the spread in the range values is caused by 1) neutron emission from the compound $Ga^{67}$ nuclei giving rise to a rather large energy spread of the ions, 2) straggling in the gas, 3) target thickness, 4) breadth of aluminium pieces, and 5) diffusion of the thermalized ions.

The contributions from the three last sources are small and will not be further discussed.

According to theory, the straggling increases with increasing mass number of the stopping gas, no matter whether the stopping is due predominantly to nuclear or to electronic collisions. This is also borne out by the experiments, as may be seen from Fig. 10.

LINDHARD and SCHARFF give the formula

$$\frac{\sigma^2}{R'^2} = \frac{2}{3}\frac{m_1 m_2}{(m_1 + m_2)^2}$$

where $\sigma$ is the standard deviation in range to be expected if the stopping were due entirely to nuclear collisions, and R′ is the average path length. The values A for the full width at half maximum height in per cent of the mean range, as obtained from this formula and by putting the average path length equal to $\left(1 + \frac{1}{3}\frac{m_2}{m_1}\right)$ times the mean range are given in Table 6.

The experimentally found total half widths B are also given and furthermore the values $C = \sqrt{B^2 - A^2}$. The relative uncertainty in the B-values may be estimated to about $4\%$. Then the uncertainties in the C-values are the figures given in the table.

If A were the correct scattering half-widths, C would be the partial half-widths resulting from other sources, i. e., essentially from neutron emission. Then, since the energy distribution resulting from this process does not

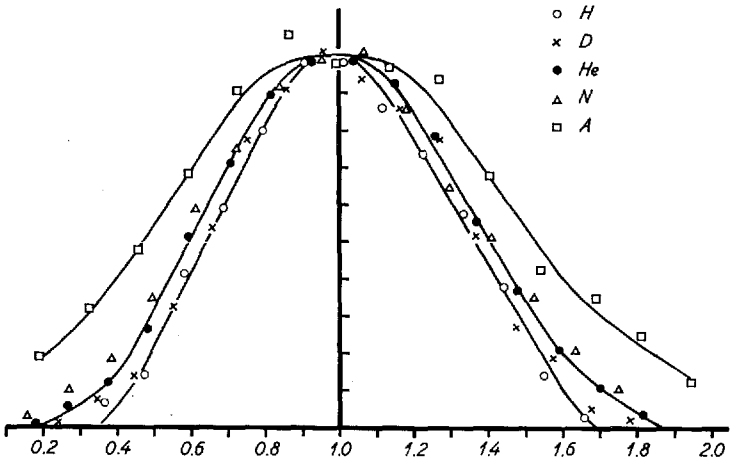


Fig. 10. Range distributions of $Ga^{66}$ ions in gases. Ordinate: relative number of particles per unit interval of range. Abscissa: range in units of the mean range $R_0$. The $Ga^{66}$ ions were produced by 19.6 MeV $\alpha$-particles on Cu. Experimental points are given for $H_2$, $D_2$, He, $N_2$, and A. Curves are only drawn for $H_2$, He, and A.

depend on the gas, and since in each gas the range is proportional to the energy, the relative half widths C should be the same in all gases (not necessarily for all $\alpha$-energies, see later). This is true within the experimental error for the light gases $H_2$, $D_2$, and He, whereas for $N_2$ the C-values come out too small, and for argon the experimental half widths are smaller than the A-values. This is not surprising; it merely shows once more that the electronic stopping cannot be neglected, and since the electronic collisions contribute less to the straggling than do the nuclear encounters, the real relative scattering half widths are smaller than the A-values.

For hydrogen the straggling is small compared to the range spread caused by neutron emission. As a first approximation, we may neglect the former and consider the value $B_H$ as a measure for the latter. For the other gases the values $D = \sqrt{B^2 - B_H^2}$ will then represent the scattering half widths, the approximation being best for the heavy gases.

TABLE 6. Full width at half maximum height of range distribution in per cent of the mean range.
B are experimental values. For the meaning af A, C, and D, see text.

| | | $E_\alpha = 19.6$ MeV | | | $E_\alpha = 13$ MeV | | | $E_\alpha = 10$ MeV | | |
|---|---|---|---|---|---|---|---|---|---|---|
| | A | B | C | D | B | C | D | B | C | D |
| $H_2$ | 23 | 68 | $64 \pm 3$ | (0) | 67 | $63 \pm 3$ | (0) | 63 | $59 \pm 3$ | (0) |
| $D_2$ | 32 | 72 | $65 \pm 3$ | (24) | 72 | $65 \pm 3$ | (26) | 70 | $63 \pm 3$ | (32) |
| He | 45 | 81 | $68 \pm 3$ | $45 \pm 8$ | 84 | $59 \pm 4$ | $32 \pm 12$ | 76 | $62 \pm 4$ | $44 \pm 8$ |
| $N_2$ | 78 | 85 | (33) | $51 \pm 7$ | 89 | (43) | $58 \pm 6$ | 88 | (41) | $62 \pm 6$ |
| A | 112 | 106 | | $81 \pm 6$ | 104 | | $79 \pm 6$ | 104 | | $83 \pm 5$ |

We may ask, what should be the shape of the range spectrum if it is determined entirely by neutron emission? We shall make the two simplifying assumptions, (I) that the neutrons are emitted isotropically in the C.M. system and, (II) that the relative number of neutrons per unit interval of energy is given by

$$\frac{dn}{dE} = C_1 E e^{-\frac{E}{T}},$$

where $C_1$ is a constant and T, the nuclear temperature of the residual $Ga^{66}$ nucleus, is also a constant [9) 10) 11)].

Introducing the momentum $P = \sqrt{2ME}$, where M is the neutron mass, gives

$$\frac{dn}{dP} = C_2 P^3 e^{-\frac{P^2}{2MT}},$$

where $C_2$ is a new constant. In this formula, $\frac{dP}{dn}$ may also stand for the number of recoil ions per unit interval of momentum. Denoting by Q the projection of P on the beam direction (see Fig. 11), the distribution in Q is given by

$$\frac{dn}{dQ}\,dQ = \iint \frac{\frac{dn}{dP}\,dP}{4\pi P^2\,dP}\, r\,d\varphi\,dr\,dQ = dQ \int \frac{\frac{dn}{dP}}{2P^2}\, r\,dr,$$

where $\varphi$ is the azimuthal angle. From Fig. 11 we get $P^2 = Q^2 + r^2$, hence for a fixed Q: $rdr = PdP$, thus

$$\frac{dn}{dQ} = \frac{C_2}{2} \int_{P=|Q|}^{P=\infty} P^2 e^{-\frac{P^2}{2MT}}\,dP.$$

Let $Q_0$ denote the momentum in the laboratory system, due to center of mass motion. The projection of the lab. momentum is $Q+Q_0$. Introducing the assumption, which is justified from the previous results, that, (III), the projection R of the range*, is given by

$$R = C_3 (Q+Q_0)^2,$$

where $C_3$ is a constant, one finds

$$\frac{dn}{dR} = \frac{\frac{dn}{dQ}}{\frac{dR}{dQ}} = \frac{C_4}{Q+Q_0} \int_{P=|Q|}^{P=\infty} P^2 e^{-\frac{P^2}{2MT}} dP. \tag{6}$$

Fig. 12 shows curves corresponding to T = 1 MeV and T = 2 MeV, respectively. The experimental points show a thin target distribution in $H_2$; the arrows on the points on the left side of the peak indicate corrections

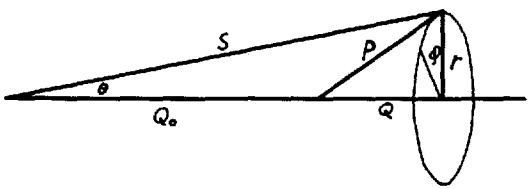


Fig. 11.

for the finite target thickness. As may be seen, the points are not inconsistent with a nuclear temperature between 1 and 2 MeV. In this region of the periodic system, and using α-particles of about 20 MeV, a nuclear temperature of about 1.2 MeV may be expected[9) 10) 11)]. Taking into consideration other contributions to the width (straggling in the target foil, finite breadth of collector foils) it is not surprising that the experimental points seem to indicate a somewhat higher temperature.

The calculated curves show a strong asymmetry. Of course, many effects will tend to remove this, but it is actually found that the experimental curves are also asymmetric, being steeper at the left than at the right side. It may be noted, however, that the points on the calculated curves in half maximum height lie closely symmetrical. The experimental value of $R_0$ was determined not from the position of the maximum activity, but as the mean of the two

* Since the projection angle $\theta$ is only small, it is not of much importance whether we talk about the range itself or its projection.

abscissae corresponding to half maximum intensity. $R_0$ thus determined is actually the range of $Ga^{66}$ nuclei corresponding to the emission of neutrons with zero momentum in the forward direction, i. e. the range of $Ga^{66}$ nuclei with a velocity equal to that of the compound nuclei. Thus, no correction should be applied for the difference between some of the ranges and their projections.

From Table 6 it may be seen that the width of the range distribution is

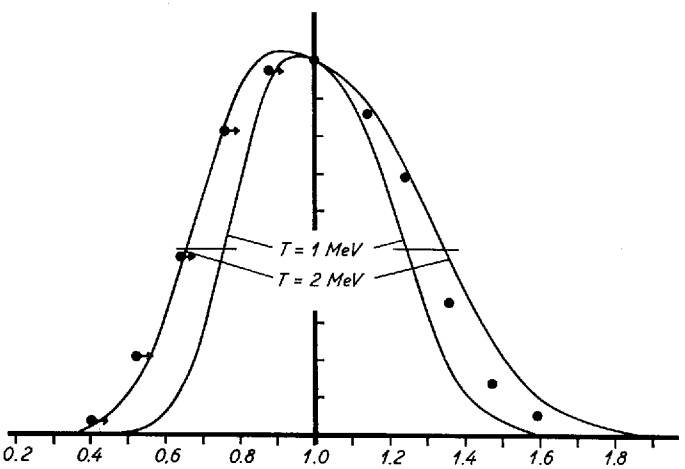


Fig. 12. Calculated curves showing the range distributions corresponding to temperatures of the $Ga^{66}$ nucleus of 1 and 2 MeV, respectively. The points are an experimental distribution obtained in $H_2$ using $\alpha$-particles with 19.6 MeV. Abscissa: range in units of $R_0$, the latter being the range corresponding to emission of a neutron with zero velocity component in the forward direction. Ordinate: relative number of particles per unit interval of range.

almost independent of the $\alpha$-energy. This indicates that the nuclear temperature decreases with decreasing $\alpha$-energy, a result which is in conformity with earlier observations[10, 11].

On the same assumptions (I) and (II), the angular distribution of the $Ga^{66}$ ions is given by

$$\frac{dn}{d\theta} = C \sin\theta \cos\theta \int_{x_1}^{\infty} x^2 e^{-x^3} dx \qquad (7)$$

where $x_1 = 2\sqrt{\frac{E_\alpha}{T}}$ and where C is a constant.

In Fig. 5 (p. 12) curves a, b, and c correspond to T = 1.6, 1.8, and 2.0 MeV, respectively, and the experimental points agree fairly well. However, the compound scattering in the target foil may be responsible for a very

considerable part of the angular width. Due to the circular geometry contributions from $\alpha$-beam divergence ($< \pm 0.°5$) and finite target diameter are small.

These experiments were carried out at the Institute for Theoretical Physics, University of Copenhagen. It is a great pleasure to express our heartiest and most deepfelt gratitude to the Director of the Institute, Professor NIELS BOHR. For valuable discussions our thanks are due the late Dr. M. SCHARFF. We thank Mr. A. HEDEGAARD for preparing the target layers, Mr. PH. DAM for operating the cyclotron, Mr. FL. DALL and Mr. CLIVE LARSEN for help in the counting and the numerical calculations, and Mr. H. CHRISTENSEN for manifold and valuable help.

## References


1. NIELS BOHR and J. LINDHARD: Mat. Fys. Medd. Dan. Vid. Selsk. **28**, no. 7 (1954).
2. NIELS BOHR: Mat. Fys. Medd. Dan. Vid. Selsk. **18**, no. 8 (1948).
3. N. O. LASSEN: Mat. Fys. Medd. Dan. Vid. Selsk. **26**, no. 5 (1950).
4. N. O. LASSEN: Mat. Fys. Medd. Dan. Vid. Selsk. **25**, no. 11 (1949).
5. J. K. BØGGILD, H. ARRØE, and TH. SIGURGEIRSSON: Phys. Rev. **71**, 281 (1947).
6. BERNARD G. HARVEY, PAUL F. DONOVAN, JOHN R. MORTON, and ERNEST W. VALYOCSIK: UCRL. 8618, p. 17 (1959).
7. TYNDALL and POWELL: Proc. Roy. Soc. London. A. **136**, 145 (1932).
8. J. LINDHARD and M. SCHARFF: Phys. Rev. **124**, 128, (1961), and paper to be published.
9. H. W. FULBRIGHT, N. O. LASSEN, and N. O. ROY POULSEN: Mat. Fys. Medd. Dan. Vid. Selsk. **31**, no. 10 (1959).
10. N. O. LASSEN and N. O. ROY POULSEN: Comptes Rendus du Congrès International, Paris 1958, p. 477 (Dunod, Paris 1959).
11. N. O. LASSEN and V. A. SIDOROV: Nucl. Phys. **19**, 579 (1960).


Indleveret til selskabet den 20. oktober 1961.
Færdig fra trykkeriet den 23. februar 1962.